STATISTICAL PROPERTIES OF THE LARGE SCALE STRUCTURES:

COSMIC SHEAR

For a review: https://arxiv.org/pdf/1201.2434.pdf (Sec 5)
https://arxiv.org/pdf/1612.06535.pdf
https://arxiv.org/pdf/0805.0139.pdf
https://arxiv.org/pdf/astro-ph/9912508.pdf

GRAVITATIONAL LENSING

Gravitational lensing: Light’s path is deflected by the gravitational potential wells of cosmic structures crossed along its journey toward us.

This leads to:

- **Change of the apparent positions of the sources**
- **Distorsion (shear) of source images**
- **Magnification of the source images**

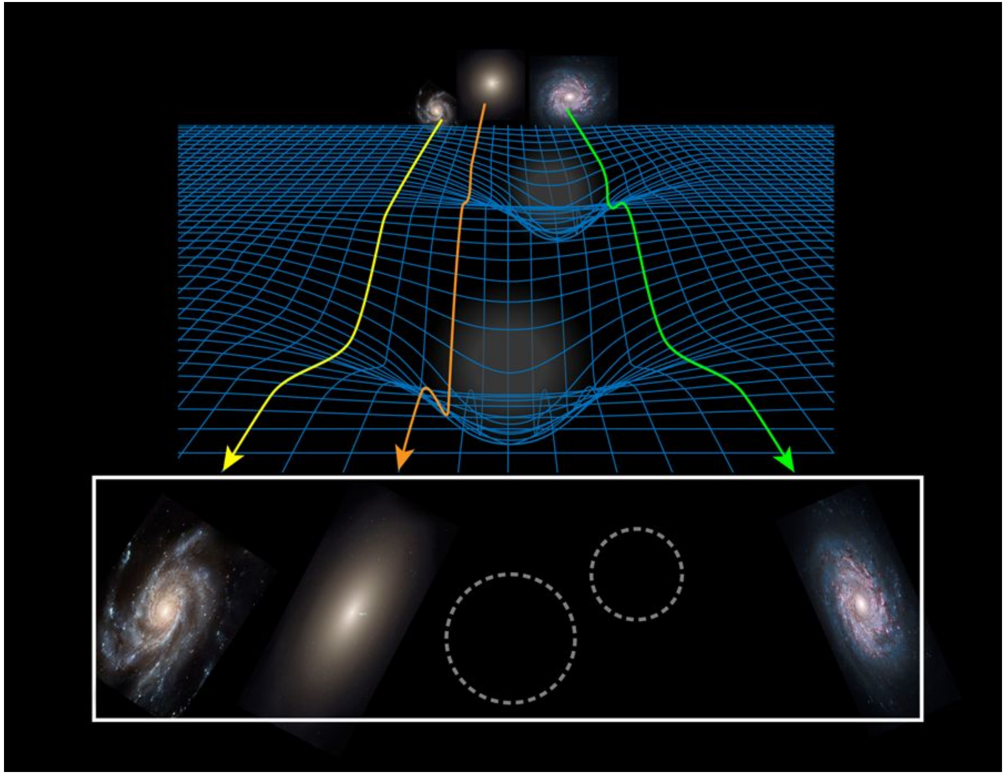

STRONG AND WEAK GRAVITATIONAL LENSING

Strong lensing:

- **Multiple images of the same source**
- **Strong distortions and magnification**

Weak lensing:

- **Shape distorted, stretched or magnified**
- **Detectable only statistically**

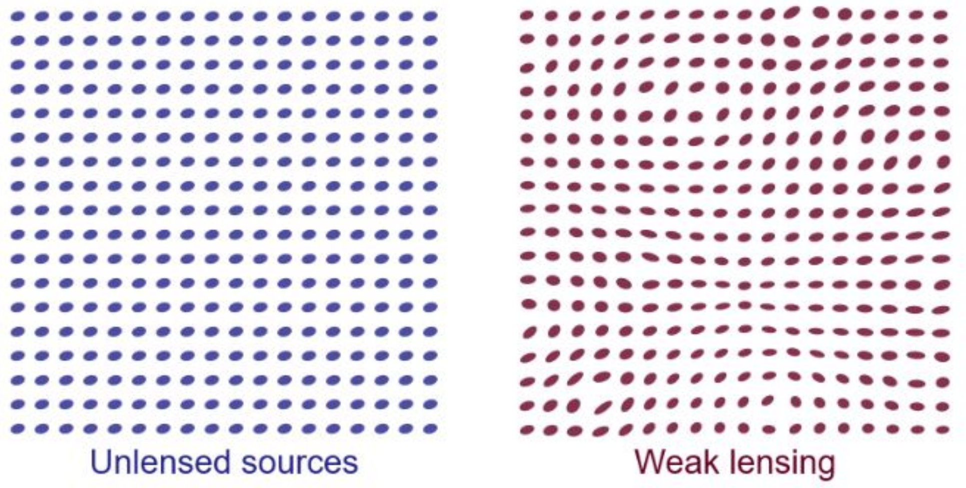

GRAVITATIONAL LENSING: LENS EQUATION

- **Deflection of light ray by a gravitational potential fluctuation Φ:**

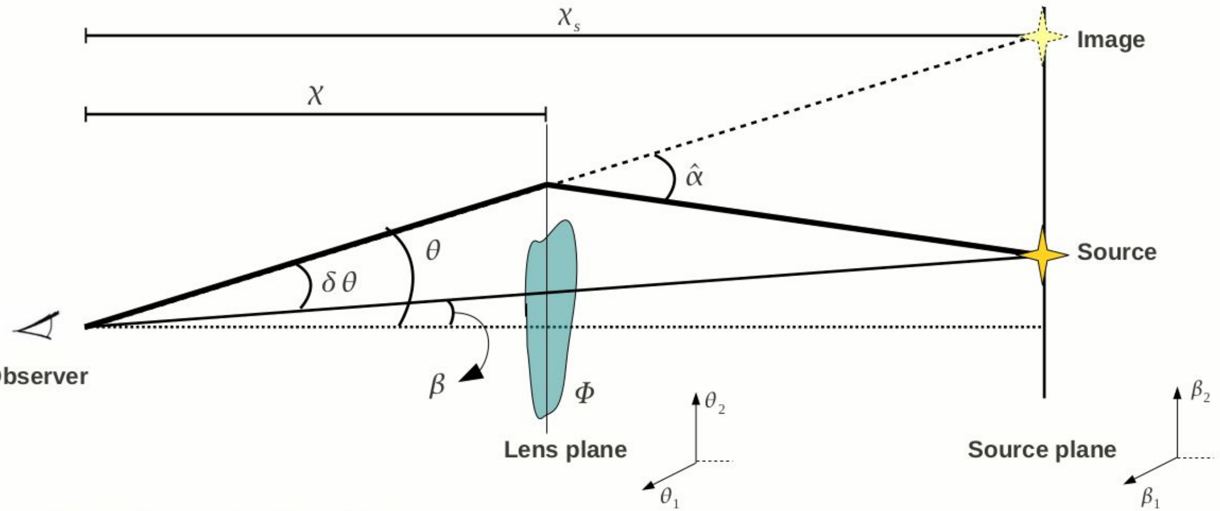

- **Using small angles approximation:**

$$\vec{\beta}\,\mathcal{D}(\chi_s)=\vec{\theta}\,\mathcal{D}(\chi_s)-\vec{\hat{\alpha}}\,\mathcal{D}(\chi_s-\chi)$$

- **Lens equation:**

$$\vec{\beta}=\vec{\theta}-\delta\vec{\theta} \qquad \text{with:} \quad \delta\vec{\theta}=\frac{\mathcal{D}(\chi_s-\chi)}{\mathcal{D}(\chi_s)}\vec{\hat{\alpha}}$$

(Scaled deflection angle)

GRAVITATIONAL LENSING: LENS EQUATION

- **Perturbed metric:**

$$ds^2=\left(1+\frac{2\Phi}{c^2}\right)c^2dt^2-a^2(t)\left[\left(1-\frac{2\Phi}{c^2}\right)\left(d\chi^2+\mathcal{D}^2(\chi)\,d\Omega^2\right)\right]$$

n **refractive index**

Weak field approximation

- **Deflection angle:**

$$\vec{\hat{\alpha}}=\frac{2}{c^2}\int\nabla_\perp\Phi(\chi)\,d\chi$$

Thin lens approximation

Born approximation

- **Deflection angle of light ray arising from all the potential gradients between obs and source:**

$$\delta\vec{\theta}=\vec{\theta}-\vec{\beta}=\frac{2}{c^2}\int_0^{\chi_s}d\chi\,\frac{\mathcal{D}(\chi_s-\chi)}{\mathcal{D}(\chi_s)}\nabla_\perp\Phi(\chi)$$

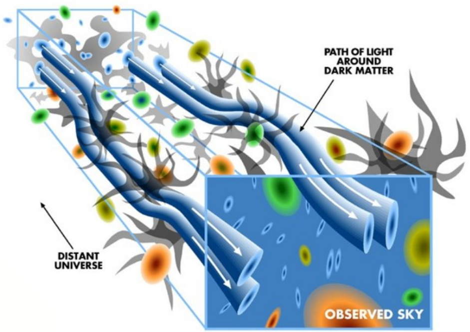

- **Deflection potential:**

$$\psi(\vec{\theta},\chi_s)=\frac{2}{c^2}\int_0^{\chi_s}d\chi'\,\frac{\mathcal{D}(\chi_s-\chi)}{\mathcal{D}(\chi_s)\mathcal{D}(\chi)}\Phi(\mathcal{D}(\chi)\vec{\theta},\chi)$$

GRAVITATIONAL LENSING: κ and γ

- **Mapping of source image:**

Conservation of surface brightness

$$I(\vec{\theta}) = I^s(\vec{\beta}(\vec{\theta})) = I^s\left[\vec{\beta}(\vec{\theta}_0) + \mathcal{A}(\vec{\theta}_0)\cdot(\vec{\theta}-\vec{\theta}_0)\right]$$

Linearized lens mapping (Jacobi matrix):

$$\mathcal{A}(\vec{\theta}) = \frac{\partial \vec{\beta}}{\partial \vec{\theta}} = \left(\delta_{i,j} - \frac{\partial^2 \psi(\vec{\theta})}{\partial \theta_i \partial \theta_j}\right) = \begin{pmatrix} 1-\kappa-\gamma_1 & -\gamma_2 \\ -\gamma_2 & 1-\kappa+\gamma_1 \end{pmatrix} =$$

$$= (1-\kappa)\begin{pmatrix} 1-g_1 & -g_2 \\ -g_2 & 1+g_1 \end{pmatrix} \quad \text{with} \quad g(\boldsymbol{\theta}) = \frac{\gamma(\boldsymbol{\theta})}{[1-\kappa(\boldsymbol{\theta})]}$$

Convergence

$$\kappa = \frac{\psi_{,11}+\psi_{,22}}{2} = \frac{\nabla^2 \psi}{2}$$

Shear

$$\gamma = \gamma_1 + i\gamma_2 = |\gamma|\, e^{2i\varphi}$$

$$\gamma_1 = \frac{\psi_{,11}-\psi_{,22}}{2} \; ; \; \gamma_2 = \psi_{,12}$$

- **Distortion of a circular image:**

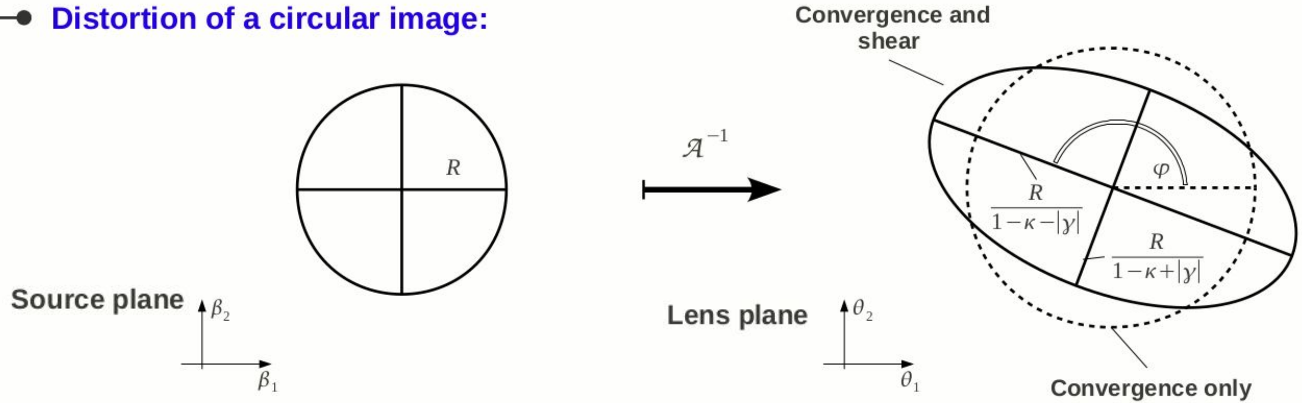

COSMIC SHEAR

From Hoekstra & Jain 2008

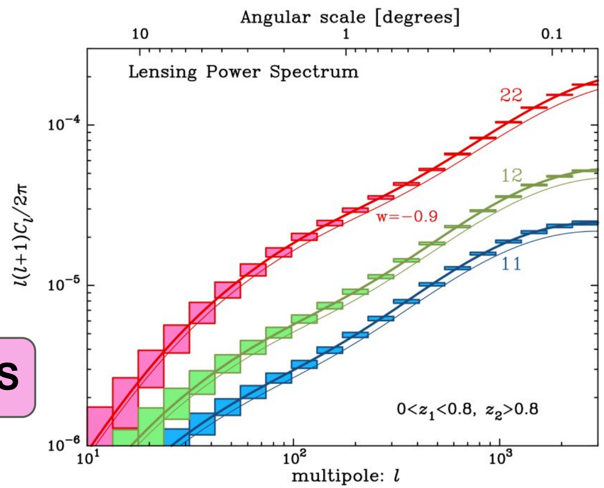

Cosmic shear denotes tiny shape distortions (weak lensing) of distant galaxy images that arise from gravitational lensing of light by the LSS of the Universe.

The coherent distortion of background images (shear) can be related to the underlying matter density distribution:

$$\kappa(\vec{\vartheta}) = \int_0^{\chi_{\max}} d\chi \, W(\chi) \, \delta(D_A(\chi)\vec{\vartheta}, \chi)$$

Integral along the LOS

Angular convergence (or shear) power spectrum

$$C_{ij}(\ell) = \frac{\langle \hat{\kappa}(\boldsymbol{\ell})\hat{\kappa}^*(\boldsymbol{\ell}')\rangle}{(2\pi)^2\delta^D(\boldsymbol{\ell}-\boldsymbol{\ell}')} = \frac{\langle \hat{\gamma}(\boldsymbol{\ell})\hat{\gamma}^*(\boldsymbol{\ell})\rangle}{(2\pi)^2\delta^D(\boldsymbol{\ell}-\boldsymbol{\ell}')} = \int_0^{\chi_{\max}} d\chi \frac{W_i(\chi)W_j(\chi)}{D_A(\chi)^2} P_\delta\left(\frac{\ell}{D_A(\chi)}, \chi\right)$$

Lens efficiency, which depends on the geometry system

Matter power spectrum

COSMIC SHEAR MEASUREMENT

The cosmic shear signal can be measured only statistically correlating the ellipticities of a large number of galaxies.

Second order cosmic shear measures:

Defining tangential and cross shear:

$$\gamma_t = -\Re[\gamma e^{-i2\phi}], \quad \gamma_\times = -\Im[\gamma e^{-i2\phi}]$$

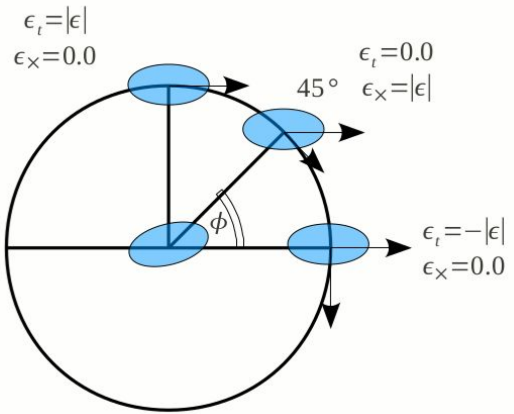

Rotationally invariant shear correlation function:

$$\xi_\pm(\theta) = \langle \gamma_t \gamma_t \rangle(\theta) \pm \langle \gamma_\times \gamma_\times \rangle, \quad \xi_\times(\theta) = \langle \gamma_t \gamma_\times \rangle(\theta)$$

Due to parity symmetry: $\xi_\times(\theta) = 0$

Relation with the power spectrum P_k:

$$\xi_\pm(\theta) = \int_0^\infty \frac{d\ell\,\ell}{2\pi} J_{0,4}(\ell\theta) P_\kappa(\ell)$$

$$P_\kappa(\ell) = 2\pi \int_0^\infty d\theta\,\theta\,\xi_\pm J_{0,4}(\ell\theta)$$

COSMIC SHEAR MEASUREMENT

The observed ellipticity of a galaxy, ϵ , is the result of the sum of its intrinsic ellipticity, ϵ^s , and the shear distortion, γ:

$$\xi_\pm = \langle \epsilon_i \epsilon_j^* \rangle = \xi_\pm^{lens} + \langle \epsilon_i^{(s)} \epsilon_j^{(s)*} \rangle + \langle \gamma_i \epsilon_j^{(s)*} \rangle + \langle \epsilon_i^{(s)} \gamma_j^* \rangle, \qquad \text{with } z_i < z_j$$

Cosmic shear signal | Intrinsic alignment | ≡0 | Shape-shear correlation

- **Intrinsic alignments : Close pair of galaxies could be aligned by tidal forces of the DM structure surrounding them.**
- **Shape-shear correlation (Hirata & Seljak 2004): DM structure (gray) causes the alignment of nearby galaxy (blue) and contributes to the lensing signal of a background galaxy (red).**

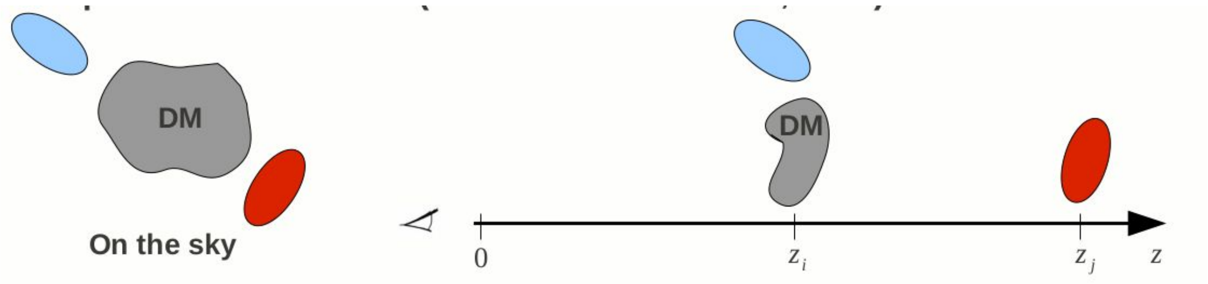

COSMIC SHEAR MEASUREMENT

The "forward" process of the source image:

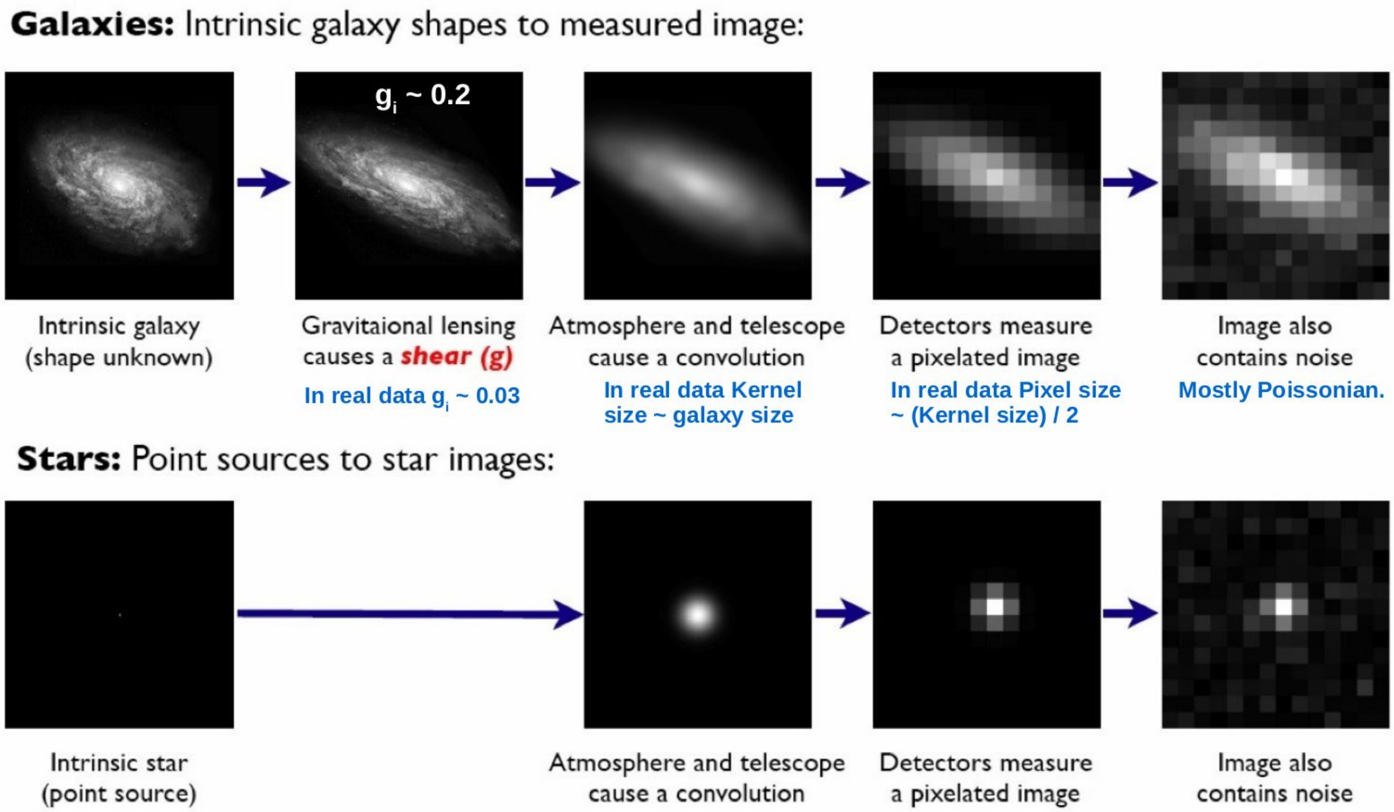

COSMIC SHEAR MEASUREMENT

The "forward" process of the source image:

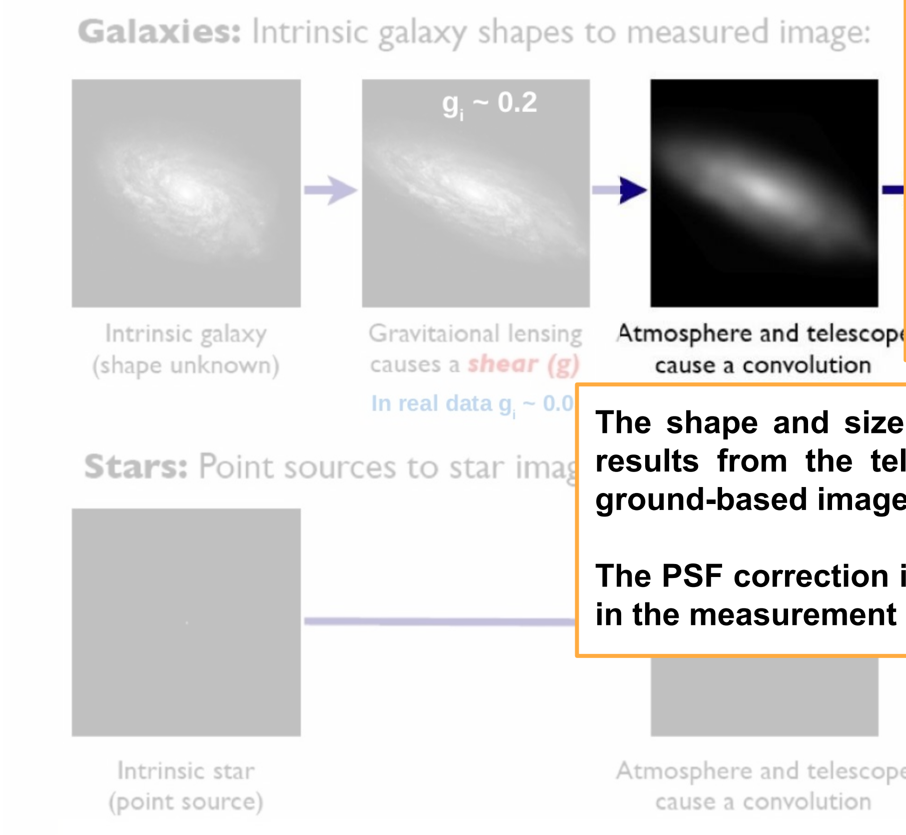

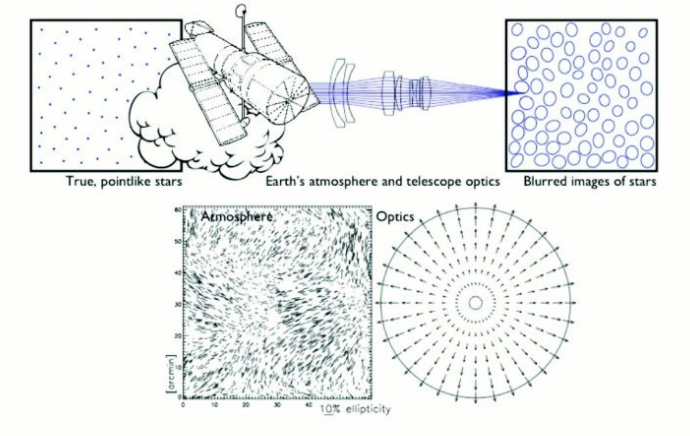

The shape and size of images are affected by the PSF, which results from the telescope optics, bed focusing, etc. and for ground-based images, from atmospheric turbulence.

The PSF correction is the most difficult, yet most important step in the measurement of lensing signal.

COSMIC SHEAR MEASUREMENT

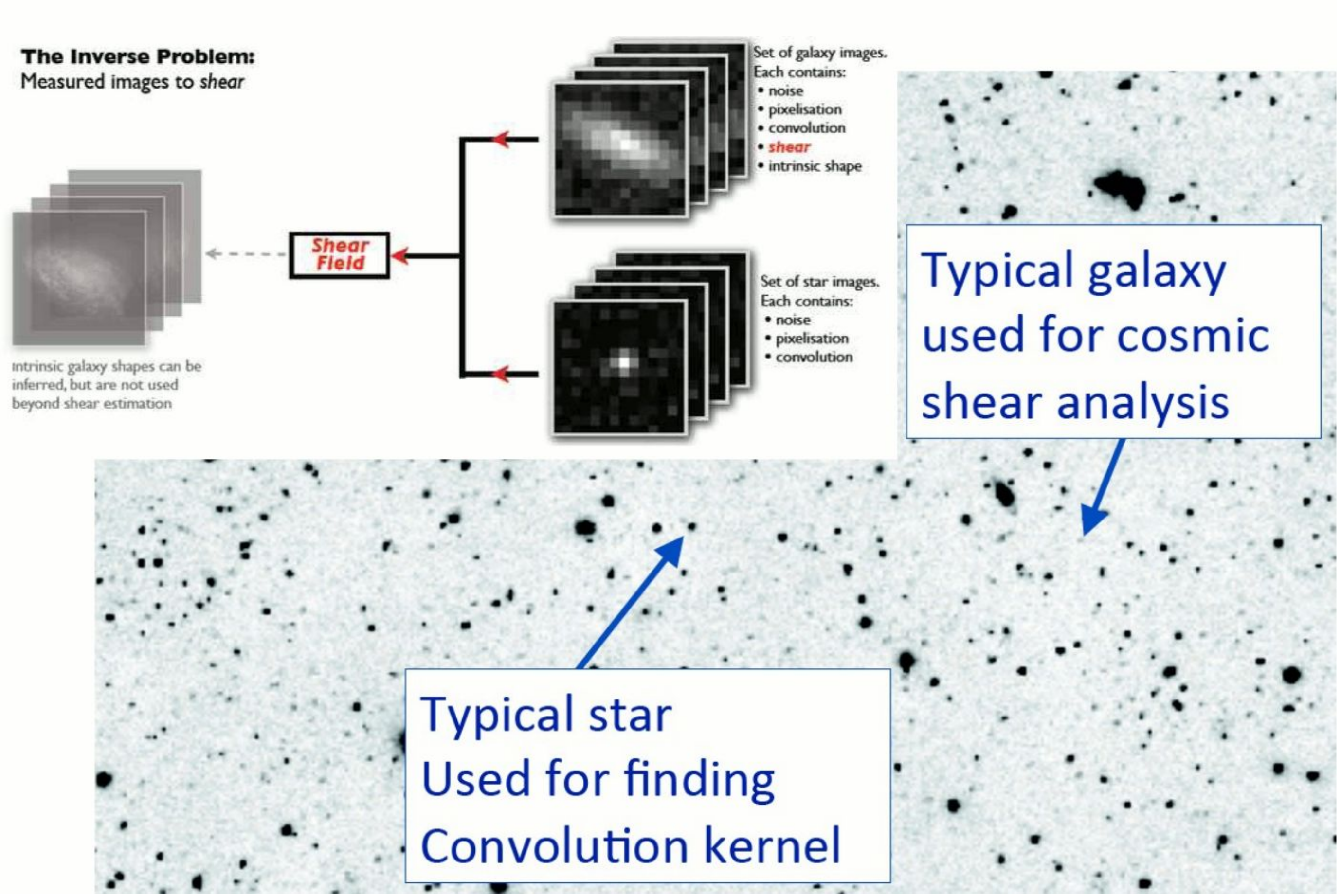

COSMIC SHEAR COSMOLOGY

Cosmic Shear:

- **Map the matter distribution directly (no assumption about the relation between DM and baryonic matter)**
- **Lensing measurements are sensitive to the geometry and provide measures of the growth of LSS → powerful probe of DE and modified gravity theories**
- **It helps in breaking parameter degeneracies when combined with other cosmological probes**

First detection of cosmic shear in 2000 by four independent groups (Bacon et al. 2000; Kaiser et al. 2000; van Waerbeke et al.; Wittman et al. 2000) using ~10^5 galaxies, 1 deg^2.
Current results from >10^8 galaxies over a few 10^3 deg^2.

Weak lensing mass map with redMaPPer clusters derived from DES Y3 shear catalogue of 100,204,026 galaxies in 4143 deg^2.

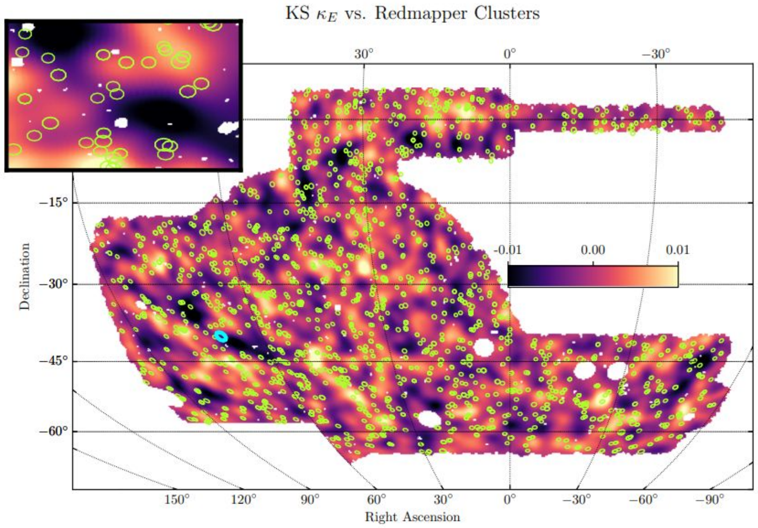

COSMIC SHEAR COSMOLOGY

Cosmic Shear:

- **Map the matter distribution directly (no assumption about the relation between DM and baryonic matter)**
- **Lensing measurements are sensitive to the geometry and provide measures of the growth of LSS → powerful probe of DE and modified gravity theories**
- **It helps in breaking parameter degeneracies when combined with other cosmological probes**

First detection of cosmic shear in 2000 by four independent groups (Bacon et al. 2000; Kaiser et al. 2000; van Waerbeke et al.; Wittman et al. 2000) using ~10^5 galaxies, 1 deg^2.
Current results from >10^8 galaxies over a few 10^3 deg^2.

DES Y3 + KIDS-1000 Shear result

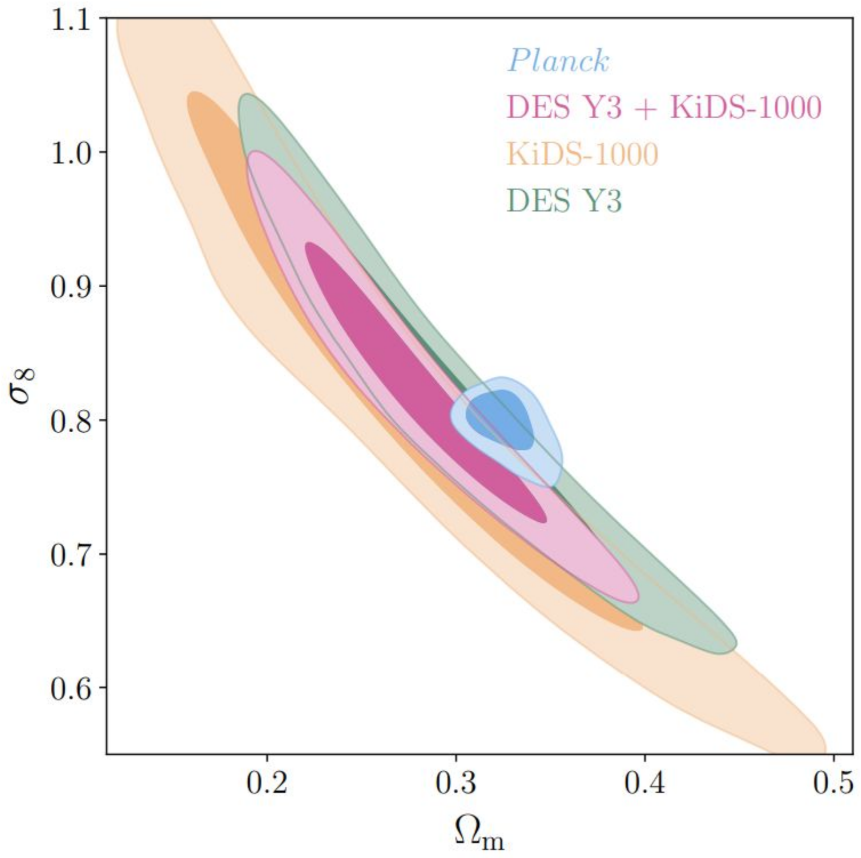

https://arxiv.org/pdf/2305.17173.pdf

CMB LENSING POWER SPECTRUM

CMB lensing effect leaves subtle imprints in the temperature and polarization anisotropies, which can be used to reconstruct a map of the lensing potential whose gradient determines the lensing deflections. For example, in propagating through a large overdense clump of matter on the line of sight, angular structures in the CMB get magnified appearing bigger on the sky. Essentially, by looking how the typical size of hot and cold spots in the CMB temperature map vary across the sky, we can reconstruct the lensing deflections and hence the integrated distribution of dark matter.

The lensing map provides a new cosmological observable, similar to maps of cosmic shear estimated from the shapes of galaxies. Its power spectrum (see below) provides access to cosmological parameters from the CMB alone that affect the late-time expansion and geometry of the Universe, and the growth of structure — parameters that have only degenerate effects in the primary CMB anisotropies.

The lensing map reconstructed from the Planck 2018 data

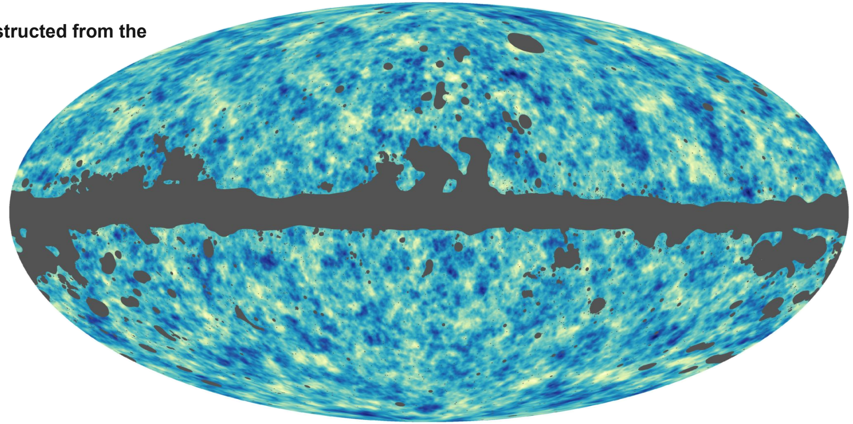

Power spectrum of the CMB lensing potential estimated from the 4-point function (trispectrum) of the Planck 2018 temperature and polarization maps (pink boxes), compared with the theoretical expectation for the LCDM model with parameters determined from the Planck measurements of the CMB power spectra.

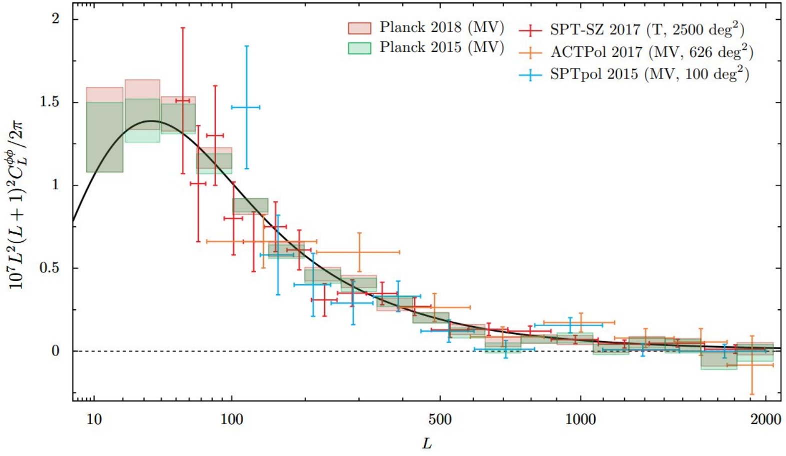

MULTI-PROBE COSMOLOGY AND CROSS-CORRELATION

In the last decade it becomes clear that combining different probes of the LSS could greatly improve the constraining power at the expense of a more complicated modeling. In particular, if we combine different tracers of the same matter density field, they will exhibit covariance (e.g. in an area where the density of galaxies is high at some redshift, the distortion of background objects by gravitational lensing will also be greater). We can measure the degree of covariance between a cosmological observable; these cross-correlation functions can provide information not given by each observable on its own (see e.g. https://lss.fnal.gov/archive/2013/pub/fermilab-pub-13-441-a.pdf).

Cross Angular Power Spectrum of two tracers *a* and *b* :

$$\langle a_{\ell m} b^*_{\ell m} \rangle \equiv C^{ab} \delta_{\ell\ell'} \delta_{mm'}$$

Primordial matter power spectrum

$$C_\ell^{ab} = 4\pi \int_0^\infty \frac{dk}{k} \mathcal{P}_\Phi(k) \Delta_\ell^a(k) \Delta_\ell^b(k)$$

Transfer functions of the tracers (e.g. galaxy, lensing, cluster)

MULTI-PROBE COSMOLOGY: 3x2pt

- **The combination of galaxy clustering, cosmic shear, and galaxy–galaxy lensing measurements – the so called 3x2pt analysis – has proven to provide powerful constraints on the structure formation in the late universe, while self calibrating many astrophysical (e.g. galaxy bias) or systematic parameters (e.g. intrinsic alignments and photo-z errors) in the model.**

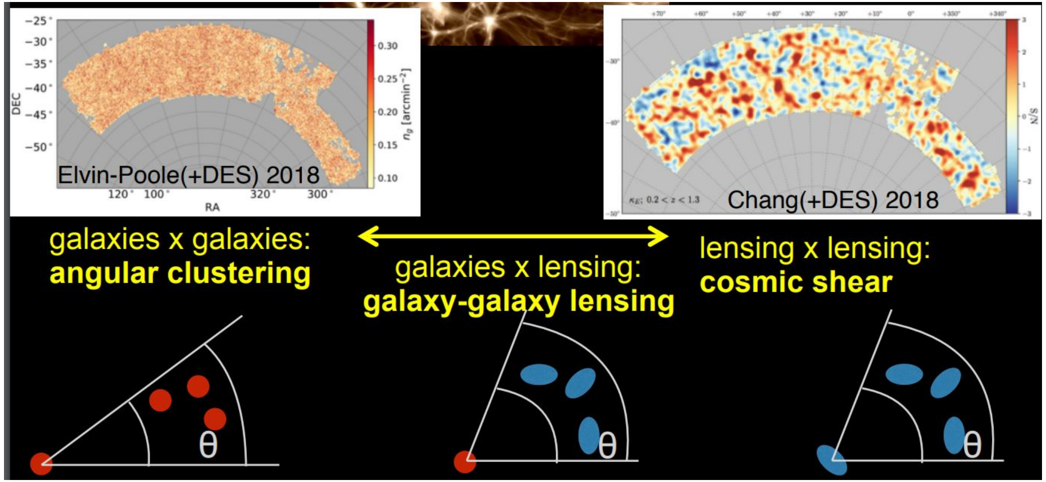

DES Y3 3x2pt analysis

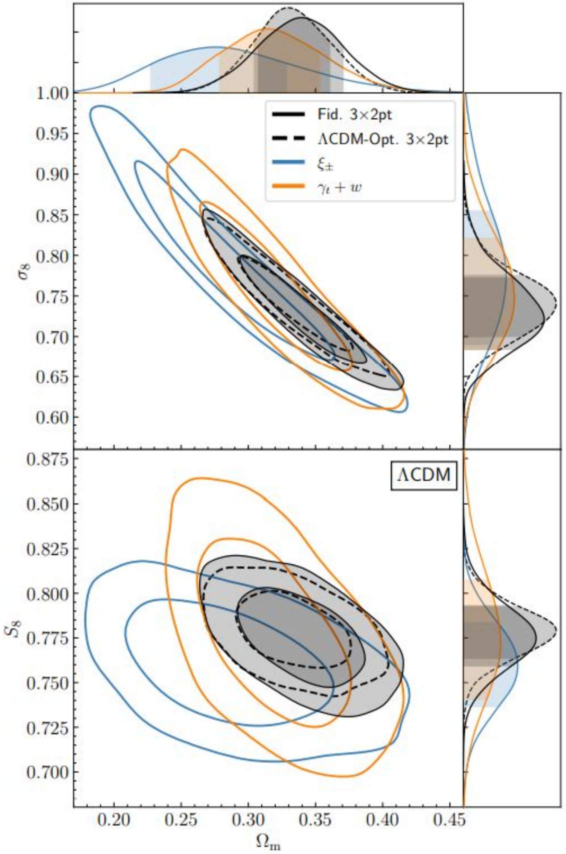

https://arxiv.org/pdf/2105.13549.pdf

MULTI-PROBE COSMOLOGY: 6x2pt+N

- **The cosmological constraints can be further improved (at the expense of a more complicated model), by including galaxy clusters abundance and auto-cross correlation functions:**

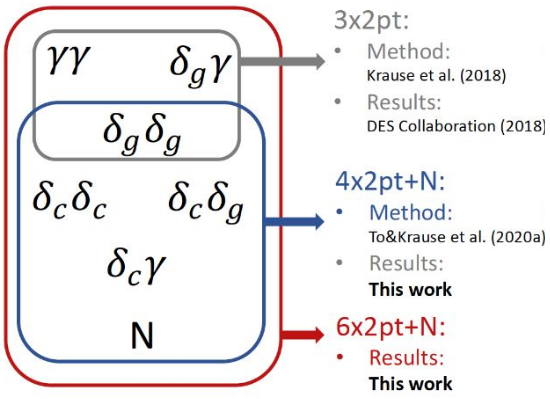

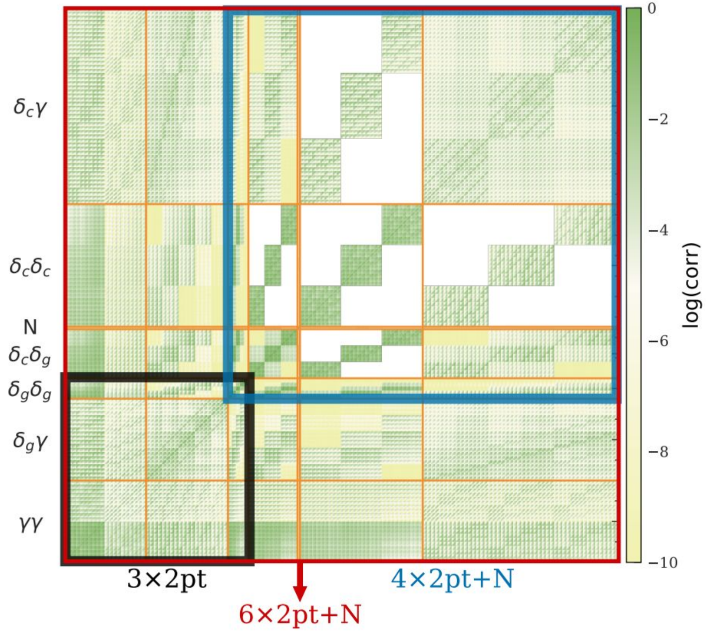

Correlation matrix for the combined analysis of galaxy, lensing and cluster correlation function and cluster counts

DES Y1 6x2pt+N analysis

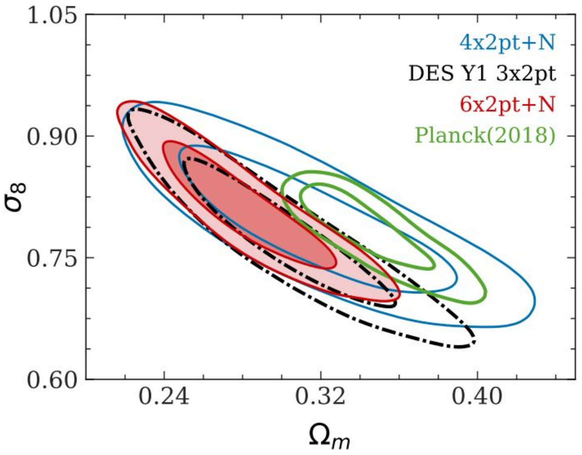

To et al 2021

TIME DELAY COSMOGRAPHY

For a review: https://link.springer.com/article/10.1007/s00159-022-00145-y

MULTIPLE IMAGES FROM STRONG LENSING

Multiply imaged time-variable sources can be used to measure absolute distances as a function of redshifts and thus determine cosmological parameters, chiefly the Hubble Constant H_0.

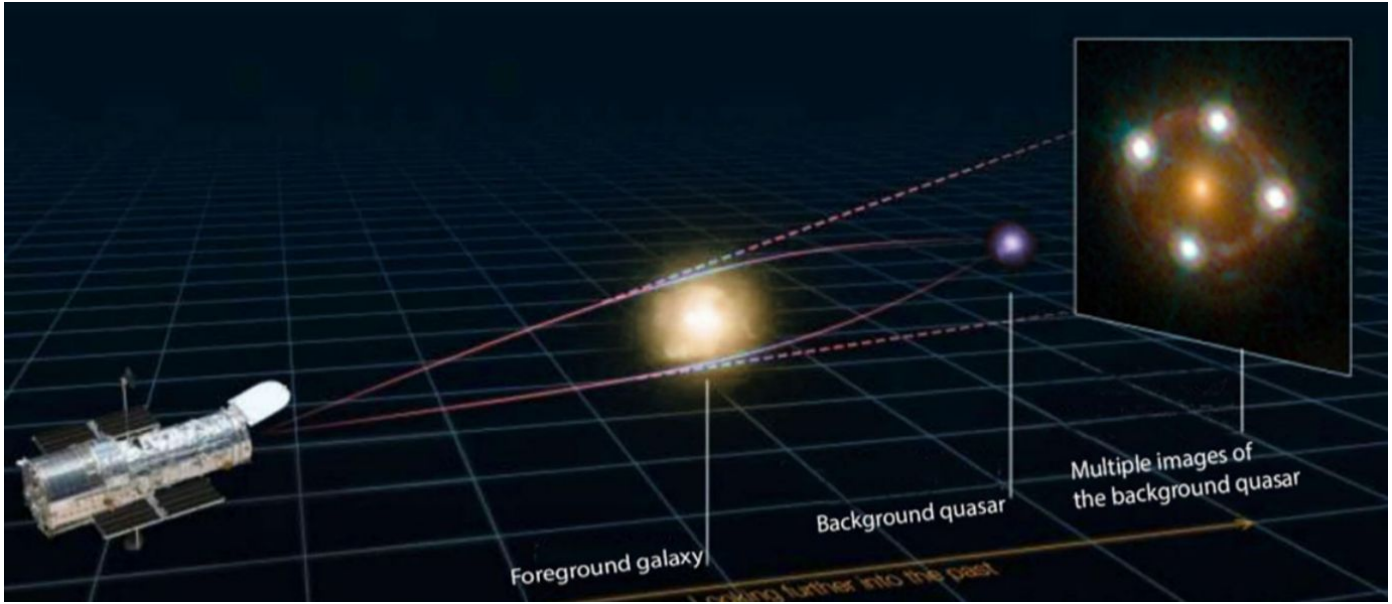

When a distant variable source (e.g., a supernova or a quasar) is multiply imaged by a foreground mass distribution (e.g., a galaxy or cluster of galaxies), the multiple images appear offset in time to the observer. The delay(s) between the leading image and trailing one(s) arise from the combination of two effects. The first one is the difference in length of the optical paths. The second is a general relativistic effect, called the Shapiro (1964) delay, owing to the difference in gravitational potential experienced by the photons along the paths.

TIME DELAY COSMOGRAPHY

The time delay between image A and image B is given by:

$$\Delta\tau_{\mathrm{AB}} = \frac{D_{\Delta\mathrm{t}}}{c}\Delta\Phi_{\mathrm{AB}}$$

$$D_{\Delta\mathrm{t}} \equiv (1+z_{\mathrm{d}})\frac{D_{\mathrm{d}}D_{\mathrm{s}}}{D_{\mathrm{ds}}}$$

$\Delta\,\phi$: Fermat potential difference between two image position. It can be predicted given a model for the mass distribution of the lens, along with the deflection angle:

$$\phi = \frac{1}{2}(\theta-\beta)^2 - \psi(\theta)$$

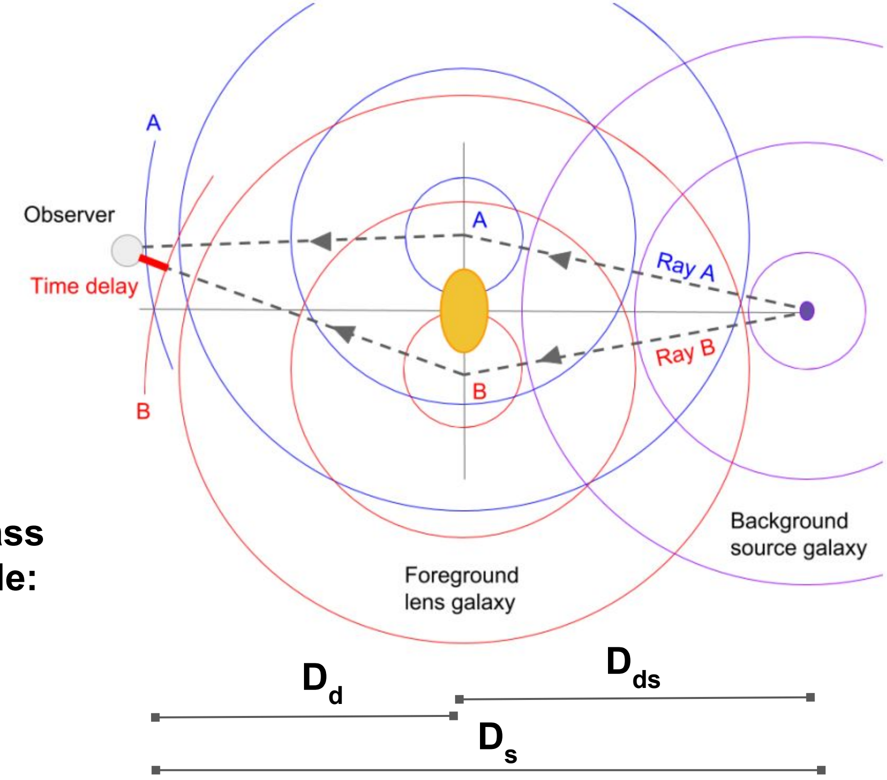

TIME DELAY COSMOGRAPHY

Steps:

- **Measure the time-delay between two images**
  - **The basic idea is to detect variations in the brightness of the quasar images in a lens system and use these variations to determine the time delay between the multiple images, given that the intrinsic brightness variations of the quasar manifest in each of the multiple images.**
- **Measure and model the potential**
- **Infer the time delay distance $D_{\Delta t}$**
- **Convert it into cosmological parameters**

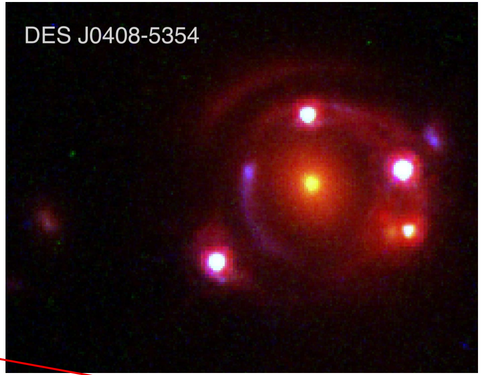

H0 measurements of 6 lensed quasars from the H0LiCOW program

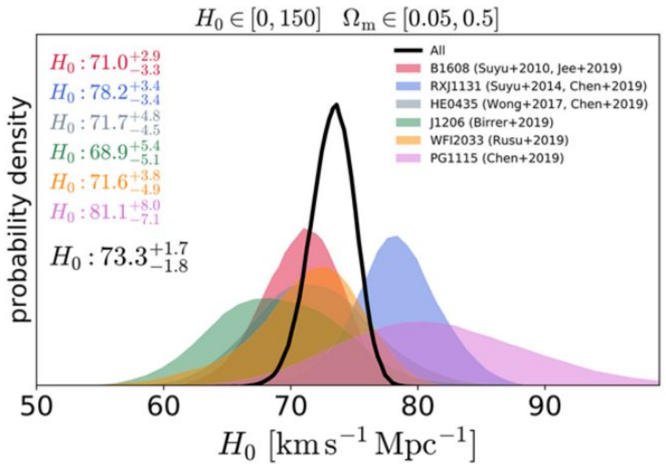

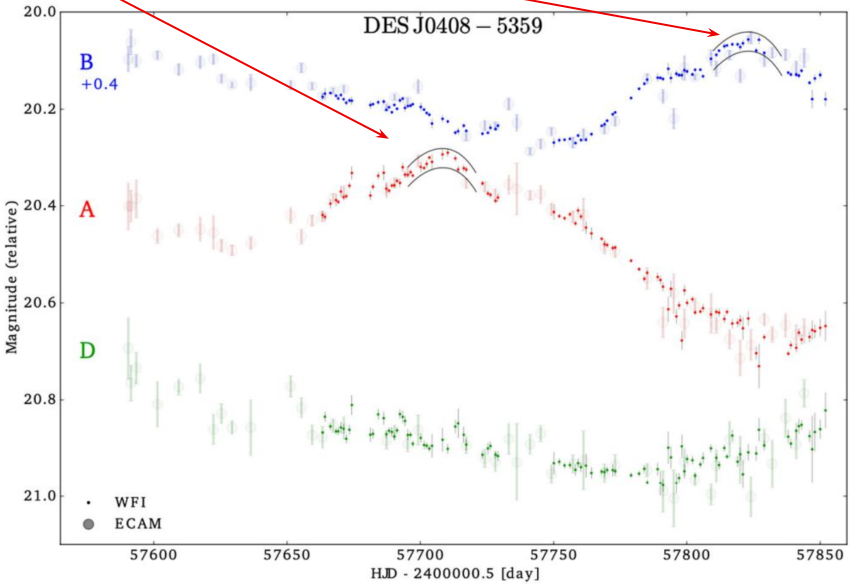

STATISTICAL PROPERTIES OF THE LARGE SCALE STRUCTURES:

LYMAN-α FOREST

For a review: https://arxiv.org/pdf/1512.00086.pdf

THE LYMAN-α FOREST

Absorption spectra of distant luminous quasars (QSOs) provide a means to probe the properties of the intergalactic medium at high redshift through the analysis of the so called Ly-α forest.
The UV light of a distant quasar – in the wavelengths blue-wards of the Ly-α emission line, $\lambda < 1216$Å – traversing the IGM towards the observer could be absorbed by intervening bunches of neutral hydrogen atoms once the photons are redshifted – due to cosmic expansion – to the proper transition frequency. The Ly-α forest, that is the series of absorption features observed in QSOs spectra at wavelengths corresponding to $1216\,(1 + z_a)$ Å, where z_a is the redshift of the absorbers, can be used to map the distribution of the IGM, which is a biased tracer of the underlying DM distribution.
Therefore, the clustering statistics of the flux can be used to constrain the shape and amplitude of the matter power spectrum and measure the structure growth at redshifts $2<z<6$, a redshift inaccessible to other LSS probes such as cosmic shear or clusters.

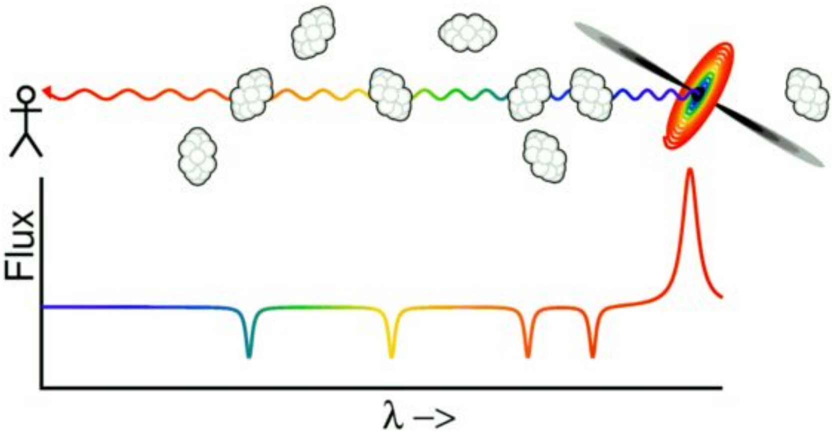

THE LYMAN-α FOREST

Ly-α optical depth:

$$\tau_{\mathrm{Ly}\alpha}(z) = 1.3\,\Delta_b \left(\frac{x_{\mathrm{HI}}}{10^{-5}}\right)\left(\frac{1+z}{4}\right)^{3/2}\left(\frac{dv/dx}{H(z)/(1+z)}\right)^{-1}$$

∝ Baryon density

Fraction of neutral hydrogen

The "trees" in the forest are the highly photoionized sheets, filaments, and halos that result from cosmic structure formation

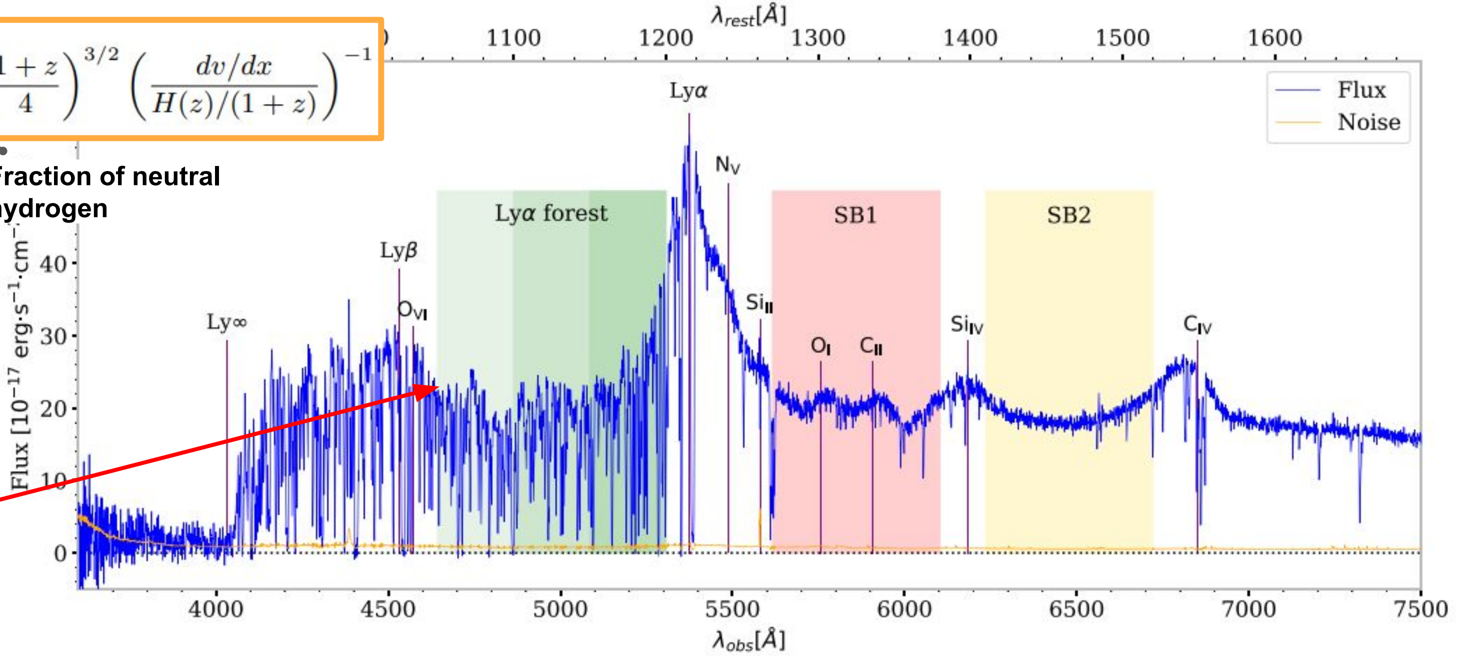

Figure 1. A particularly high-signal spectrum of a quasar located at a redshift $z = 3.42$ measured by DESI with an exposure time of 2300 s. This quasar was observed on 2021 April 12, in the SV3 programme, on DESI tile 221 (TARGETID $= 39627746095137037$, RA $= 217.263°$, Dec. $= -1.755°$). The quasar flux is represented in blue and its noise in orange. The Ly α forest is shown in green. The side-band regions 1 and 2 pictured in red and yellow are used to estimate the forest contamination by metals.

THE LYMAN-α FOREST 1d POWER SPECTRUM

The fluctuations of the Ly α forest flux, δ_f = F(x)/<F(x)> -1, along the line of sight *L*, can be used to measure the one-dimensional (1D) Ly-α forest power spectrum:

$$P_F(k) \equiv \frac{|\tilde{\delta}_f(k)|^2}{L}$$

Cosmological inference from the Lyα forest spectra is complicated by there being no reliable analytic model for the mildly nonlinear densities probed by the forest. All analyses require a comparison with large cosmological simulations.

Above k ≃ 0.02 s/km sensitive to the "warmness" of the dark matter

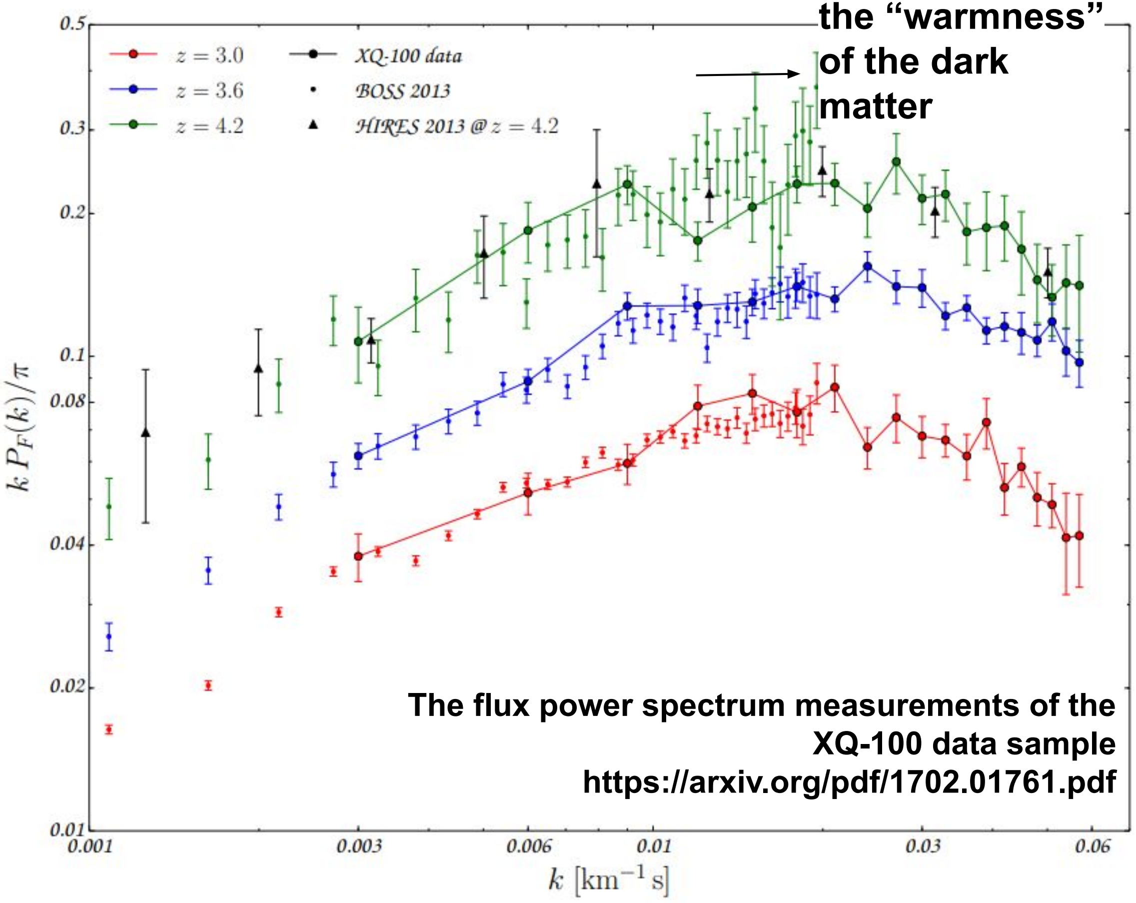

The flux power spectrum measurements of the XQ-100 data sample https://arxiv.org/pdf/1702.01761.pdf